Chemistry Europe
European Chemical Societies Publishing

WILEY VCH

Excellence in Chemistry Research

Announcing our new flagship journal

- Gold Open Access
- Publishing charges waived
- Preprints welcome
- Edited by active scientists

Meet the Editors of *ChemistryEurope*

Luisa De Cola
Università degli Studi di Milano Statale, Italy

Ive Hermans
University of Wisconsin-Madison, USA

Ken Tanaka
Tokyo Institute of Technology, Japan

Chemistry–A European Journal
Research Article
doi.org/10.1002/chem.202203580
Chemistry Europe
European Chemical Societies Publishing
www.chemeurj.org

Photophysical Characterization of Isoguanine in a Prebiotic-Like Environment

Javier Ortín-Fernández[+],[a] Naishka E. Caldero-Rodríguez[+],[b] Carlos E. Crespo-Hernández,*[b] Lara Martínez-Fernández,*[a] and Inés Corral*[a]

Abstract: It is intriguing how a mixture of organic molecules survived the prebiotic UV fluxes and evolved into the actual genetic building blocks. Scientists are trying to shed light on this issue by synthesizing nucleic acid monomers and their analogues under prebiotic Era-like conditions and by exploring their excited state dynamics. To further add to this important body of knowledge, this study discloses new insights into the photophysical properties of protonated isoguanine, an isomorph of guanine, using steady-state and femtosecond broadband transient absorption spectroscopies, and quantum mechanical calculations. Protonated isoguanine decays in ultrafast time scales following 292 nm excitation, consistently with the barrierless paths connecting the bright S_1 ($\pi\pi^*$) state with different internal conversion funnels. Complementary calculations for neutral isoguanine predict similar photophysical properties. These results demonstrate that protonated isoguanine can be considered photostable in contrast to protonated guanine, which exhibits 40-fold longer excited state lifetimes.

Introduction

Small biomolecular building blocks containing carbon, hydrogen, nitrogen, oxygen, phosphorus, and sulfur, composing the primordial soup, were intensively impacted by ultraviolet radiation during the prebiotic Era.[1,2] It has been proposed that the photochemistry/photophysics occurring at these early times could have had a significant effect on the evolution of this prebiotic mixture to the RNA nucleobases and, thus, in the composition of the first forms of RNA.[3–5] Among other photophysical properties, canonical nucleobases exhibit very efficient and ultrafast nonradiative relaxation pathways to the ground state, making them exceptionally photostable.[6,7,8] This ultrafast decay to the ground state is thought to be one of the intrinsic characteristics that allowed the survival of these molecules in the prebiotic environment.[9–12] Hence, elucidating the electronic relaxation pathways of plausible prebiotic precursors is vital to shed light into the molecular origin of life and understand the current composition of the genetic material.

In this study, we investigate the excited state relaxation mechanism of one of these prebiotic molecules, isoguanine (IsoG).[13–16] IsoG, also known as 2-hydroxyadenine, is a constitutional isomer of guanine (Gua), with an amino and a carbonyl group, respectively, occupying the C6 and C2 positions of the purine chromophore (Figure 1). It is believed that IsoG could have been present in the prebiotic environment being part of the complex mixture of canonical and non-canonical nucleobases.[3] In fact, this species was found as a side product in the reaction of the HCN tetramer with small carbon compounds to produce adenine and Gua.[17]

Beyond its putative role in the prebiotic Era, IsoG can also be naturally found in biological DNA arising from the oxidative stress of adenine,[18,19] being its yield comparable to the most frequent lesion, 8-oxoguanine.[19–21] It has also been demonstrated that certain polymerases are able to insert IsoG in an oligonucleotide forming Watson-Crick like pairs with isocytosine.[22] This unconventional non-canonical nucleobase pair is part of the Artificially Expanded Genetic Information System (AEGIS) Hachimoji alphabet[23] and has been thoroughly studied in the literature.[24] Notwithstanding the relevance of the photoproperties of IsoG, there are only a few studies available on the literature on this system. Based on resonance-enhanced multiphoton ionization, IR-UV double resonance spectroscopy, pump-probe experiments and quantum mechanical results, de Vries and coworkers propose a relaxation mechanism for the keto tautomers of IsoG in gas phase, which suggests the population of dark $n\pi^*$ states with long excited state lifetimes.[25] Recently, the excited state dynamics of IsoG nucleoside and deoxynucleoside were reported in aqueous solution at pH 1.4 and 7.4.[26] The results in this work reveal that

[a] J. Ortín-Fernández,[+] Dr. L. Martínez-Fernández, Dr. I. Corral
Departamento de Química
Universidad Autónoma de Madrid
C/Francisco Tomás y Valiente 7, 28049 Madrid (Spain)
E-mail: lara.martinez@uam.es
ines.corral@uam.es

[b] Dr. N. E. Caldero-Rodríguez,[+] Dr. C. E. Crespo-Hernández
Department of Chemistry
Case Western Reserve University
44106 Cleveland, OH (USA)
E-mail: carlos.crespo@case.edu

[+] These authors contributed equally to this work.

Supporting information for this article is available on the WWW under https://doi.org/10.1002/chem.202203580

© 2023 The Authors. Chemistry - A European Journal published by Wiley-VCH GmbH. This is an open access article under the terms of the Creative Commons Attribution Non-Commercial License, which permits use, distribution and reproduction in any medium, provided the original work is properly cited and is not used for commercial purposes.

© 2023 The Authors. Chemistry - A European Journal published by Wiley-VCH GmbH

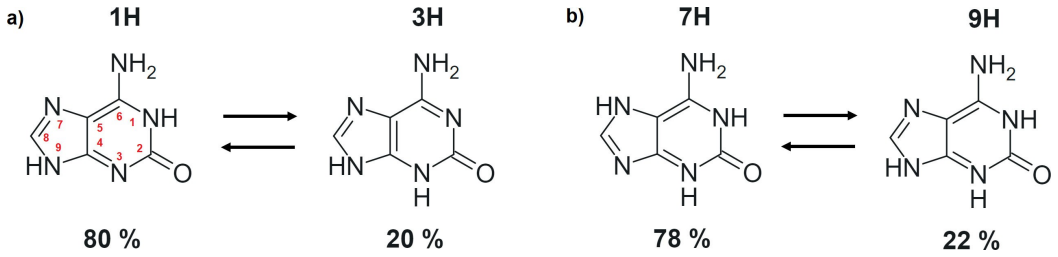

Figure 1. Most relevant tautomers of IsoG in aqueous solution and their relative abundance: (a) 1H,9H-IsoG (left, major tautomer) and 3H,9H-IsoG (right, minor tautomer) in neutral medium and (b) 1H,3H,7H-IsoG (left, major tautomer) and 1H,3H,9H-IsoG (right, minor tautomer) in acidic medium (right). Atom numbering of the purine ring is shown in red.

the protonation status of IsoG does not seem to have a large impact on the excited state dynamics of this system. However, to the best of our knowledge, there is no information available about the excited state dynamics of the free nucleobase in aqueous solution, affected by the existence of several tautomers.[27,28]

Considering the drastic pH changes and photoexcitation processes that occurred during the prebiotic Era due to the absence of the ozone layer, we have considered in this study the impact of protonation in the photodynamics of this system.[1,29,30]

Protonation processes at low pH could have had a dramatic impact on the excited state dynamics of prebiotic nucleobases,[1] turning relevant the study of their excited state dynamics under these experimental conditions. Hereby, steady-state and femtosecond broadband transient absorption spectroscopy, combined with gas phase quantum mechanical calculations, were used to elucidate the excited state relaxation pathways of the tautomeric forms of IsoG in aqueous buffer solution at pH 2.4. For completeness, the photophysics of IsoG in neutral medium has been also simulated. Experimental measurements in aqueous solutions at a neutral pH were not possible due to the poor solubility of the nucleobase under these experimental conditions.

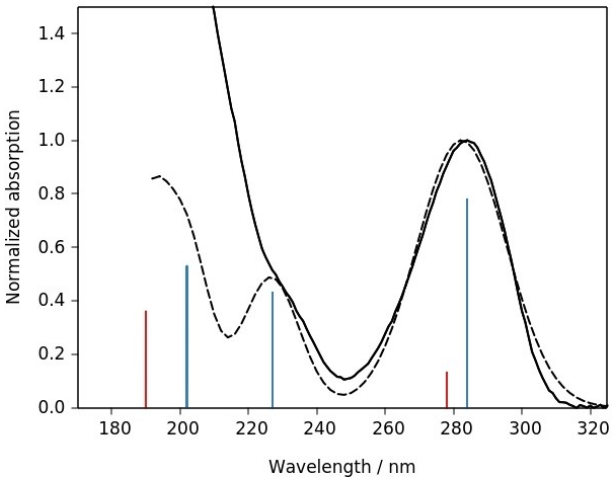

Figure 2. Normalized absorption spectrum for IsoG in aqueous buffer solution at pH 2.4 (solid line) superimposed to the gas phase convoluted MS-CASPT2 absorption spectrum considering both protonated tautomers (dashed line). 7H excitations are represented by vertical blue lines whereas red vertical lines are used for the 9H tautomer. Oscillator strengths were set relative to the normalized S_1 of 7H and weighted according to the corresponding tautomeric abundances.

Results and Discussion

Absorption spectrum

Figure 2 shows the absorption spectrum of IsoG in aqueous buffer solution at pH 2.4. It contains two absorption bands with maxima around 175 and 284 nm, which agrees with previous experimental absorption spectrum reported for IsoG in aqueous solution at pH 2.[31] Molar absorption coefficients were obtained from the work by Mason, where the maximum of the lowest energy band at 284 nm refers a value of $10.7\times10^3\ M^{-1}cm^{-1}$ (Figure S5).[32] IsoG in aqueous buffer solution at pH 2.4 can be considered non-fluorescent since a very low emission intensity was registered for this molecule, which might be affected by the sensitivity of our spectrometer. Hence, a 10^{-4} fluorescence quantum yield was estimated for IsoG in aqueous buffer solution at pH 2.4, similar to canonical nucleobases in aqueous solution.[6] The pK_a values for IsoG were reported as 4.51 and 8.99.[32,33] With these pK_a values and the Henderson-Hasselbalch relationship, it was determined that 99% of IsoG exists as the protonated species in aqueous buffer solution at pH 2.4. The tautomers available in aqueous solution under acid conditions were calculated to be the 7H and 9H keto forms of IsoG, which are the focus of this investigation.

Following the protocol described in the Computational Details section, we estimate that the relative abundance of the two tautomers 7H:9H of protonated IsoG in water solution is 78:22 (Figure 1). The comparison of the experimental and theoretical spectra in Figure 2 (see also Tables S1–S4 and Figures S1 and S2) reveals an excellent agreement for the low energy region and the number of states considered. The theoretical spectrum presents three significant absorption bands in the range from 200 to 320 nm. The lowest energy band (~280 nm) arises from the combination of the S_1 bright states (S_1 $\pi_1\pi_1^*$) (Tables S1, and S2, labelling of the orbitals follows Schemes S1–S2) of both tautomers. In addition, 7H is responsible for the shoulder at 227 nm, corresponding to the S_2

© 2023 The Authors. Chemistry - A European Journal published by Wiley-VCH GmbH

$\pi_1\pi_2^*$ state. The second band predicted experimentally below 200 nm, is due to a combination of excitations of both tautomers, where the main contributors to the red edge of the band are the S_4 $\pi_1\pi_2^*/\pi_2\pi_1^*$ excited state of 9H and the S_4 $\pi_6\pi_1^*$ excited state of 7H (Tables S1 and S2).

Deactivation pathways of protonated IsoG

The main deactivation pathways, following excited state relaxation from the Franck-Condon (FC) region, are depicted in Figure 3. Geometries of the relevant stationary points are available in the Supporting Information (Supporting Information, Figures S6–S12). As the major tautomer, the potential energy surface (PES) of 7H is discussed first. Following 292 nm irradiation, the system is expected to populate the S_1 $\pi_1\pi_1^*$ excited state (Figure 3, green path). From this point, the system will evolve to a planar minimum, $\pi_1\pi_1^*_{min1}$, with an adiabatic energy of 3.77 eV. This region of the PES is connected to a 0.40 eV more stable plateau ($\pi_1\pi_1^*_{plateau}$) compared to $\pi_1\pi_1^*_{min1}$. Structurally, this plateau involves the puckering at the C6 position, and the relocation of the NH_2 group almost perpendicular to the plane ($\delta_{C2-N1-C6-N11} = 73°$, recall Figure 1 for atom labelling). The evolution from the minimum to the plateau is smooth as revealed by the almost barrierless profile between the two regions of the PES as described by linear interpolated pathways (LIIC) calculations. A barrierless profile was found to connect the plateau with the S_1 $\pi_1\pi_1^*/S_0$ internal conversion funnel, IC_a.

For completeness, we have also explored the deactivation mechanism involving the puckering at the C2 position (Figure 3, purple path); a typical decay coordinate in nucleobases and nucleobase derivatives.[33] A S_1 $\pi_1\pi_2^*/S_0$ conical intersection was located at 4.07 eV, IC_c. The topology of this region of the PES was found to be planar and thus the system is expected to be retained in this region ($\pi_1\pi_2^*_{plateau}$) before internally converting to the ground state. Access to this plateau is direct from the FC region, when the system approaches the S_2 $\pi_1\pi_2^*/S_1$ $\pi_1\pi_1^*$ internal conversion funnel (IC_b) characterized by a dihedral angle of $\delta_{C6-N1-C2-O10} = 66°$.

Finally, the possibility of deactivation through the triplet manifold from the singlet minimum was also considered. Although the triplet state, T_1 $\pi_1\pi_1^*$, lies close in energy at the position of the $\pi\pi^*$ minimum, the computed Spin-Orbit Coupling (SOC) is negligible ($< 1\ cm^{-1}$), in agreement with the El-Sayed rules.[34,35] We found no triplet states with $n_O\pi_1^*$ character in an energy range of 2 eV around the minimum position. We succeeded in optimizing a S_1 $\pi_1\pi_1^*/T_2$ $n_O\pi_1^*$ intersystem crossing (ISC) funnel with a strong coupling between the singlet $\pi\pi^*$ and the T_2 (SOC of 60 cm^{-1}), however, its energy, relative to the S_1 $\pi_1\pi_1^*$ minimum (+0.53 eV), is significantly high for this crossing to be efficient upon excitation at 292 nm. Notwithstanding, should part of the excited population reach the triplet manifold through this crossing, the population would decay to a very stable T_1 minimum (Figure S16 of the Supporting Information).

The deactivation potential energy profile for the 9H tautomer can also be found in Figure 3 (values in parenthesis). Compared to 7H, two additional $\pi_1\pi_1^*_{min2}$ and $\pi_1\pi_2^*_{min3}$ minima were found at the position of the plateaus localized for 7H. Also interesting, the IC funnels to the ground state (IC_a and IC_c) and energy barrier to access the C2 puckering deactivation route (IC_b) were found to lie systematically higher for the 9H tautomer.

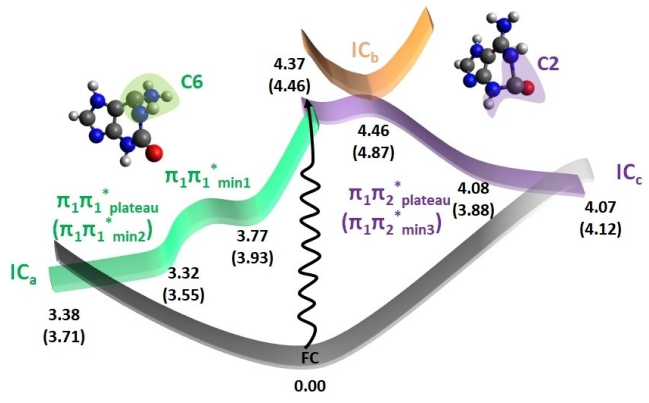

Figure 3. Schematic potential energy profile along the coordinates relevant to the relaxation process for 7H and 9H tautomers of IsoG (the data for the 9H tautomer is shown in parenthesis). Energies were set relative to the ground state minimum in eV.

Femtosecond transient absorption spectroscopy

Figure 4 presents broadband transient absorption spectroscopy measurements performed for protonated IsoG upon 292 nm excitation. The formation of two transient bands, with maxima at 400 and 600 nm, is observed within the cross-correlation of the pump and probe beams (Figure 4a). During the initial 0.47 ps, an increase in intensity is observed for the transient band at 400 nm with a simultaneous blueshift to ca. 385 nm. This is accompanied by a decrease in the amplitude for the lower-energy band with a maximum at 600 nm, forming an apparent isosbestic point around 490 nm (Figure 4b). After 0.47 ps, the amplitude of the higher-energy band decreases and slightly blueshifts around 10 nm. The transient bands decay until no absorption signal is observed at ca. 4 ps within the sensitivity of the spectrometer used (Figure 4c).

The transient absorption data of protonated IsoG was fitted (350–700 nm) with a two-component sequential model, using a Gaussian instrument response function with a full width at a half maximum (FWHM) of 200 fs (Figure 5). Lifetimes of (0.33 ± 0.06) and (0.83 ± 0.01) ps and evolution associated difference spectra (EADS) were obtained. Several studies show that vibrational cooling is often probe-wavelength dependent, with shorter wavelengths presenting longer lifetimes than the longer wavelengths.[36,37,38,39] In this study, the possibility of observing vibrational cooling in the ground state has been ruled out since the analysis suggests that the longer decay signal is not probe-wavelength dependent. It is important to point out that the solvent signal has a small contribution to the initial dynamics at

© 2023 The Authors. Chemistry - A European Journal published by Wiley-VCH GmbH

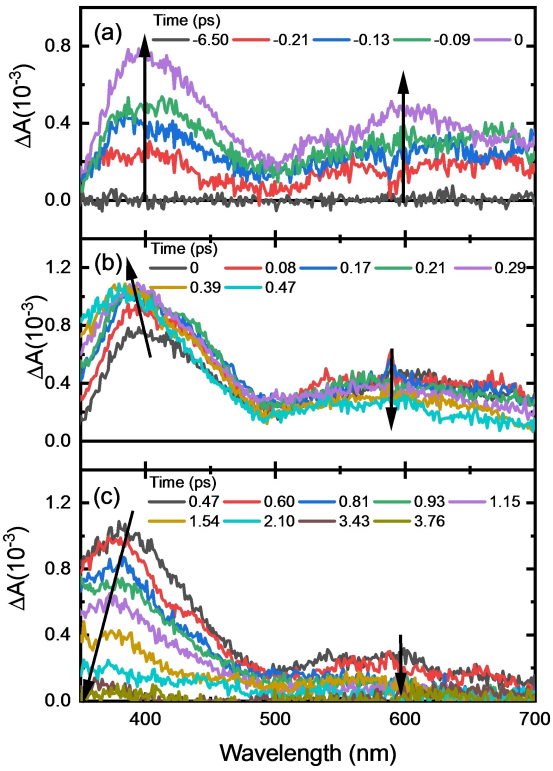

Figure 4. Evolution of the transient absorption spectra of IsoG in aqueous buffer solution at pH 2.4, following 292 nm excitation. Time zero was determined at the maximum amplitude of absorption (panel a) within the cross-correlation of the pump and probe beams. Black arrows show the evolution of the transient absorption spectra in each panel. Note that the overtone of the excitation beam is observed around 584 nm. However, its amplitude is small enough not to significantly affect the global analysis performed for the transient data.

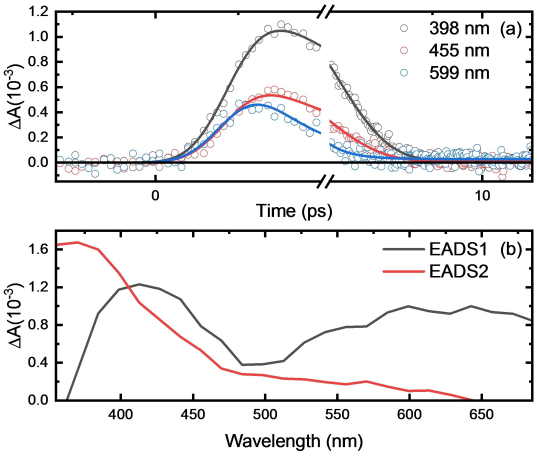

Figure 5. (a) Representative decay traces of IsoG in aqueous buffer solution at pH 2.4. The solid lines correspond to the best fit obtained from a global analysis of the transient absorption data in a 350 to 700 nm region. Note that the abscissa is linear until 1.2 ps, after which a log scale is used. (b) Evolution associated difference spectra (EADS) for the protonated IsoG in the probe spectral range between 350 to 700 nm.

probe wavelengths below ca. 350 nm (< 0.4 ps); for this reason, this region was not considered during the data analysis.

The computed excited state absorption (ESA) spectra at each stationary point for the main tautomer, 7H, are depicted in Figure 6a. The ESA for $\pi_1\pi_1^*{}_{min1}$ presents two absorption bands of similar intensity peaking at the red-edge of the spectrum, i.e., at 500 and > 700 nm; whereas the $\pi_1\pi_1^*{}_{plateau}$ has only a main band more into the blue at ~420 nm. For its part, the absorbance of $\pi_1\pi_2^*{}_{plateau}$ is less important, but could also residually contribute to the experimental spectra both in the red and the blue-sides. The ESA for the $\pi_1\pi_1^*{}_{min1}$ of the minor tautomer, 9H (Figure 6b), also presents two bands, but are blueshifted with respect to 7H, in agreement with the observed trend in the FC region. For 9H, only $\pi_1\pi_1^*{}_{min1}$ and $\pi_1\pi_1^*{}_{min2}$ were considered in the simulations since the barrier to access $\pi_1\pi_2^*{}_{min3}$ lies considerably higher in energy.

Photophysics of neutral IsoG

For completeness, the PES of the tautomers of IsoG in neutral medium was also studied. Please recall that the lack of solubility of this nucleobase in neutral medium prevented us from obtaining experimental results. Neutral IsoG presents two important tautomers (Figure 1, left): 1H,9H-isoguanine (1H) and 3H,9H-isoguanine (3H) with relative abundances 80:20.[40] The gas phase theoretical absorption spectrum of neutral IsoG, accounting for the two most abundant tautomers, is shown in Figure 7 (see also Tables S5–S8 and Figures S3 and S4). The two least energetic bands correspond to the bright states of the two tautomers, S_1 $\pi_1\pi_1^*$, peaking at 305 and 258 nm for the major and minor tautomer, respectively. Near the UV-C range, two additional bands appear, ascribed to the S_4 $\pi_3\pi_1^*$ of 1H, almost three times as intense as the S_2 $\pi_1\pi_2^*$ of 3H, which peak at 197 and 212 nm, respectively. In general, we observe that the MS-CASPT2 spectra is moderately blue shifted compared to the ADC(2) results of de Vries and coworkers, and that ADC(2) produces an stabilization of the $n_O\pi^*$ state by 0.6 eV for the most stable keto tautomer.[25]

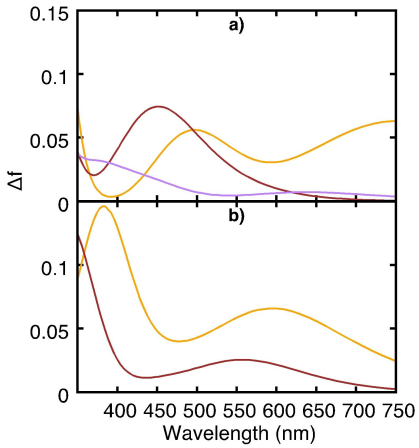

Figure 6. Computed excited state absorption (ESA) spectra for the (a) 7H and (b) 9H protonated tautomers of IsoG: $\pi_1\pi_1^*{}_{min1}$ (orange), $\pi_1\pi_1^*{}_{plateau}$ and $\pi_1\pi_1^*{}_{min2}$ (brown) and $\pi_1\pi_2^*{}_{plateau}$ (purple).

© 2023 The Authors. Chemistry - A European Journal published by Wiley-VCH GmbH

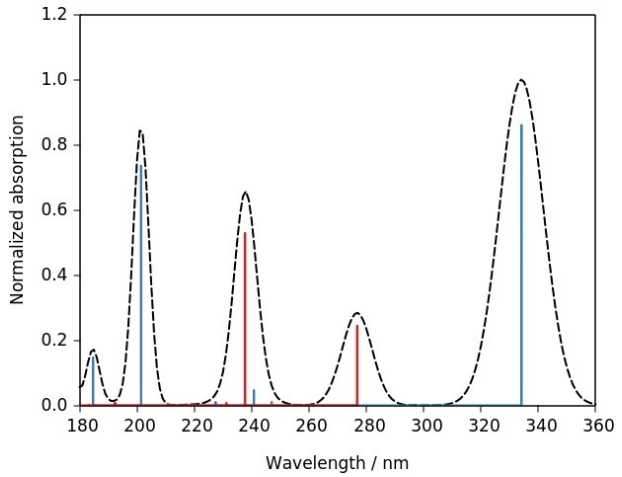

Figure 7. Normalized gas phase convoluted MS-CASPT2 theoretical absorption spectrum considering the 1H and 3H tautomers of neutral IsoG. 1H excitations are represented with vertical blue lines, whereas red vertical lines denote excitations of 3H. Oscillator strengths were set relative to the normalized S_1 of 1H and weighted according to the corresponding tautomeric abundances.

The PES relevant to the deactivation of photoexcited-1H is summarized in Figure 8. Following irradiation at 292 nm, the same wavelengths used for the protonated nucleobase, the system is expected to populate the S_1 $\pi_1\pi_1^*$ minimum, $\pi\pi^*_{min}$, lying at 3.45 eV above the ground state minimum. This minimum is not completely planar and exhibits a slight pyramidalization of the N1 position. Then, a negligible barrier ($\approx$0.05 eV) needs to be surpassed to reach a smooth down-hill region of the PES that converges into a S_1 $\pi_1\pi_1^*/S_0$ conical intersection at 3.13 eV (IC in Figure 8). This conical intersection is analogous to the IC_a of protonated IsoG and presents a puckered C6 position with the amino group lying out-of-plane ($\delta_{C2-N1-C6-N11} = 72°$).

In the case of 3H (Figure 8, in parenthesis), we also located a S_1 $\pi_1\pi_1^*$ minimum, $\pi\pi^*_{min}$, accessible from the FC region, at

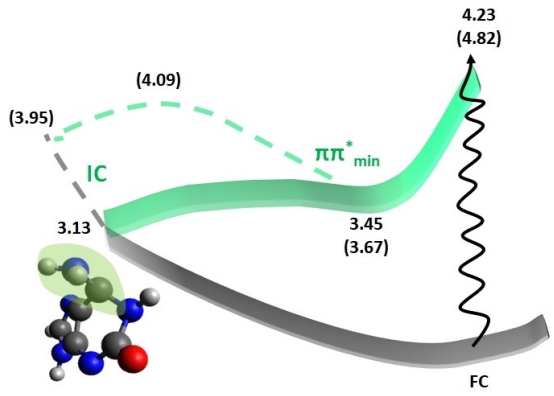

Figure 8. Schematic potential energy profile for the 1H and 3H tautomers (values for 3H in parenthesis), connecting the FC region and the C6-puckered internal conversion funnel. Energies are presented in eV relative to the ground state minimum.

3.67 eV. Compared to the 1H tautomer, this minimum presents a more important distortion of the six-membered ring, which is folded along the C6–N3 axis. Depopulation of this minimum is possible via the S_1 $\pi_1\pi_1^*/S_0$ conical intersection, which happens to be located higher in energy compared to the equivalent conical intersection for the 1H tautomer, at 3.95 eV. Accessing this funnel requires surmounting an energy barrier of 0.42 eV. In consequence, the 3H tautomer is expected to deactivate in a longer time scale compared to the 1H tautomer through this equivalent pathway. Geometries of the relevant stationary points can be found in the Supporting Information (Figures S13–S15).

Singlet-triplet population transfer was also explored as a potential deactivation route. At the S_1 $\pi_1\pi_1^*$ minima positions, no neighboring electronic triplet states strongly coupled to the singlets were found. ISCs with strong singlet-triplet SOCs (60 and 56 cm^{-1} for 1H and 3H, respectively) were located for both tautomers. However, the high energy of these funnels compared to the singlet-singlet conical intersections suggest exclusive deactivation along the singlet manifold upon excitation at 292 nm. Schemes of the triplet PES are included in the Supporting Information (Figure S16).

Discussion

Steady-state photophysics of IsoG in acidic medium

The excellent agreement between the experimental and computed absorption spectra for protonated IsoG, as shown in Figure 2, supports our computed relative abundances and the presence of both tautomers in solution. According to our simulations (Figures S1 and S2, Tables S1–S4), the least energetic band at 284 nm in the experimental absorption spectrum can be ascribed to the S_1 states of both tautomers, whereas the shoulder of the most intense band at 230 nm is attributed to the S_2 $\pi_1\pi_2^*$ excited state of 7H.

Excited state dynamics of IsoG in aqueous buffer solution at pH 2.4

Considering the theoretical and experimental results, we propose the following nonradiative relaxation mechanism for IsoG in aqueous buffer solution at pH 2.4. As previously reported for other purine derivatives,[33] the primary relaxation pathway for protonated IsoG upon excitation at 292 nm involves an ultrafast branching of the population along two reaction coordinates, which respectively evolve through the puckering of the C6 and C2 positions. The population is expected to reach in a first stage the planar $\pi_1\pi_1^*_{min1}$ minimum and partially the $\pi_1\pi_1^*_{plateau}$ and $\pi_1\pi_1^*_{min2}$ minimum with a lifetime (τ_1) of (0.33 $\pm$ 0.06) ps. In fact, the black EADS (Figure 9b), extracted from the global analysis, is perfectly reproduced by a combination of the $\pi_1\pi_1^*_{min1}$ of the 7H and 9H tautomers, with a small contribution of $\pi_1\pi_1^*_{min2}$ and $\pi_1\pi_1^*_{plateau}$ (Figure 9a). This pathway is expected to be faster for the major

© 2023 The Authors. Chemistry - A European Journal published by Wiley-VCH GmbH

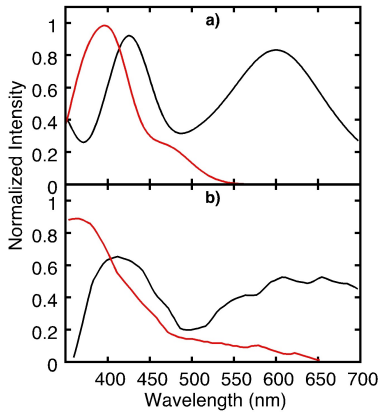

Figure 9. (a) Comparison of the simulated EADS (upper panel) obtained from the combination of 7H IsoG (70% $\pi_1\pi_1^*{}_{min1}$ + 10% $\pi_1\pi_1^*{}_{plateau}$) + 9H IsoG (15% $\pi_1\pi_1^*{}_{min1}$ + 5% $\pi_1\pi_1^*{}_{min2}$) (black) and 7H IsoG (80% $\pi_1\pi_1^*{}_{plateau}$) + 9H IsoG (20% $\pi_1\pi_1^*{}_{min2}$) (red), and **(b)** the experimental EADS (lower panel). A blue shift of 0.3 eV was applied to the simulated EADS.

tautomer and we predict an increase of this lifetime concomitant to an increment in the proportion of 9H tautomer due to the larger barrier to access IC_a for this species.

The remaining population in $\pi_1\pi_1^*{}_{min1}$ would evolve to $\pi_1\pi_1^*{}_{min2}$ and the $\pi_1\pi_1^*{}_{plateau}$ with a lifetime (τ_2) of (0.83 ± 0.01) ps. In this way, the red EADS (Figure 9b), resulting from the loss of intensity at the red-edge and a blue shift of the 400 nm signal, would be mainly described by the absorption of $\pi_1\pi_1^*{}_{min2}$ and the $\pi_1\pi_1^*{}_{plateau}$. Indeed, a linear combination of the spectra of these two points provides a good agreement between the experimental and theoretical EADS (Figure 9), even though it was necessary to apply a small blue shift to the theoretical spectrum. According to the topology calculated for the potential energy landscape of 7H, a fraction of the excited population could follow an alternative deactivation route. The part of the population accessing the S_1 with an excess of vibrational energy could overpass the small energy barrier connected to the S_2 $\pi_1\pi_2^*/S_1$ $\pi_1\pi_1^*$ internal conversion funnel (0.09 eV), IC_b, and then reach $\pi_1\pi_2^*{}_{plateau}$. From this point, the population could access the internal conversion funnel, IC_c, and decay back to the ground state. Indeed, we cannot exclude the contribution of the $\pi_1\pi_2^*{}_{plateau}$ to the transient signal since the barrier preceding its population could be overcome in the time scales registered and the ESA from this plateau presents a very weak intensity in the range of wavelengths investigated. C2 secondary deactivation, however, is not expected to play a role in the deactivation for 9H under our experimental conditions since the IC_b barrier lies 0.41 eV above the FC S_1 $\pi_1\pi_1^*$ excitation energy, making it inaccessible for the system.

The apparent isosbestic point observed in the transient absorption data of protonated IsoG in Figure 4b suggests that drastic conformational changes might be occurring to access the conical intersections to the ground state. This is confirmed by the geometrical rearrangements necessary to access the internal conversion funnels found in our simulations: IC_a presents a distorted purine ring at the C6 position and a displacement of the amino group out of the plane of the aromatic ring; and in the same line, accessing IC_c internal conversion funnel affects the oxo group at the C2 position. The experimental data suggests that the triplet excited states are not populated in IsoG under the experimental conditions considered. Consistently, the only located ISC point showing a strong S–T coupling (SOC 60 cm^{-1}), lies too high in energy to be accessed, considering the excitation wavelength used in the experiments (292 nm, 4.2 eV).

Comparison with IsoG in gas phase

To the best of our knowledge, there is only one study in the literature that partially addresses the PES of neutral IsoG.[25] We will restrict the following comparison to the 1H species, which is the only keto tautomer analyzed in the bibliography (Keto-N1,9 in Ref. [25]).

Similarly to our MS-CASPT2 results, the ADC(2)/aug-cc-pVDZ absorption spectrum for 1H presents two intense bands peaking at 317 and 231 nm with oscillator strengths of 0.141 and 0.171 respectively,[25] although the two methods predict reverse intensities.

According to the ADC(2) and NEVPT2/MRCIS(6,5) potential energy profiles calculated in Ref. [25], the photoexcited system is expected to populate a transient S_1 $n_O\pi^*$ minimum at ca. 4.0 eV that would be subsequently depopulated through the $n_O\pi^*/S_0$ conical intersection,[25] located ca. 0.5 eV above the minimum. Our MS-CASPT2 calculations, however, reveal that the ADC(2) geometry of the S_1 $n_O\pi^*$ minimum in Ref. [25] does actually not correspond to a minimum but a S_2 $n_O\pi^*/S_1$ $\pi\pi^*$ degeneracy. In fact, no $n_O\pi^*$ minimum was found in the S_1 potential in the present work.

Comparison with canonical nucleobases (Gua and $GuoH^+$)

Considering the above information regarding the photophysics and the photodynamics of IsoG in acidic and neutral media, we are now in the position to compare the photoexcited dynamics of IsoG with that of the canonical nucleobase Gua. There is an overall consensus in the computational literature that photoexcited ($\pi\pi^*L_a$) Gua in the gas phase deactivates in a barrierless manner to the ground state via the 2E conical intersection,[41,42] puckered at C2 with an out-of-plane deviated NH_2 substituent,[33] resembling the conical intersection found in this work for neutral IsoG. Although ISC has been reported along the main decay pathway of Gua, the estimated SOC is small (8 cm^{-1}),[43] and, thus, the experimentally estimated triplet quantum yield for Gua is almost negligible (0.0012).[44] Consistently, femtosecond experiments of Gua ribonucleoside and nucleotide in aqueous solution at neutral pH report a lifetime in the sub-ps regime (< 1 ps).[45] From all the above, we can conclude that the exchange of the substituents' position of Gua does not seem to severely affect the shape of the PES. Accordingly, excited state lifetimes of 3 ps were reported for 2′-deoxyisoguanosine and isoguanosine using femtosecond transient absorption spectroscopy.[26]

© 2023 The Authors. Chemistry - A European Journal published by Wiley-VCH GmbH

A very important increase in the fluorescence quantum yield (by a factor of ~400), compared to the neutral form, was registered for the protonated guanosine ($GuoH^+$) and guanosine monophosphate ($GMPH^+$),[46] with fluorescence lifetimes of 196 ± 7 ps,[47] 191 ± 4 ps,[38] or 209 ps[48] ($GuoH^+$), and 167 ps ($GMPH^+$), respectively.[46] Transient absorption measurements on $GMPH^+$ in aqueous buffer solution at pH 2 upon 287 nm excitation confirm the population of the $^1\pi\pi^*$ L_a state, with two quasi stationary points contributing to the absorption signal: L_a^{planar} and L_a min, with N7 and C8 lying out of the plane.[46] A small energy barrier needs to be overcome to transition from L_a^{planar} to L_a min, with lifetimes of $\tau_1 = 0.4$ ps and $\tau_2 = 2.3$ ps. Slow internal conversion occurs from the L_a min to the ground state in $\tau_3 = 167$ ps.[46] Thereby, IsoG decays faster than $GuoH^+$ in acidic aqueous solution. From these results, we then conclude that the exchange of oxo and NH_2 group positions in $GuoH^+$ accelerates the internal conversion process.

Conclusions

The electronic relaxation pathways of protonated IsoG in aqueous buffer solution at pH 2.4 were investigated by combining steady-state and femtosecond broadband transient absorption spectroscopies, with quantum mechanical calculations. Two tautomers are present in these experimental conditions, 7H and 9H. The S_1 potential energy surface of the two tautomers of IsoG, suggests the population in a first stage of a planar $\pi\pi^*$ minimum ($\pi_1\pi_1^*$), with partial population of a distorted $\pi\pi^*$ plateau (7H)/minimum (9H), both connected by an almost planar PES. This process has been attributed a lifetime of 0.33 ps. The evolution of the population from the minimum to the plateau occurs in 0.83 ps. The 7H tautomer presents an additional deactivation pathway that involves a different $\pi\pi^*(\pi_1\pi_2^*)$ excited state that might be either populated from internal conversion from the S_2 or along the S_1, after the access of the system to the S_2 $\pi_2\pi_1^*/S_1$ $\pi_1\pi_1^*$ region that lies close to the FC S_1 $\pi\pi^*$. Deactivation via the S_1 $\pi_2\pi_1^*/S_0$ crossing cannot be discarded for 7H, based on the collected data. The latter mechanism is energetically hindered for the minority 9H tautomer due to the 0.32 eV higher energy barrier found to access the conical intersection region. No ISC funnels were found to be energetically accessible from the populated minima or plateaus, in accordance with the experimental data.

The investigation of the deactivation mechanism of neutral IsoG suggests the decay of the major tautomer 1H via C6-puckered funnel, which is accessed in a barrierless manner from the FC region. This mechanism was found to be importantly hindered for the 3H tautomer, where a 0.42 eV energy barrier between the S_1 $\pi_1\pi_1^*$ minimum and the S_1 $\pi_1\pi_1^*/S_0$ conical intersection was located. In consequence, an ultrafast decay in the range of the subpicoseconds is expected for photoexcited 1H, whereas a slower decay would be expected for the 3H tautomer.

Overall, our experimental and theoretical results suggest that IsoG is photostable in aqueous buffer solution at pH 2.4, an essential property for the survival of this molecule in the early Earth. Calculations on neutral IsoG suggest that the 1H tautomer should be essentially photostable in a neutral environment, whereas the 3H tautomer is expected to undergo a slower deactivation. The higher fluorescence yields and the excited lifetimes of hundreds of ps reported for $GuoH^+$ monomers compared to protonated IsoG support that the latter presents a photophysical profile compatible with the minimization of photochemical processes compared to Gua under drastic acidic pH conditions. Preserving its integrity even under extreme prebiotic conditions could justify at least in part the existence of IsoG in the early Earth period. Interestingly, both neutral Gua and IsoG exhibit a similar photophysical behavior, i.e., ultrafast decay, pointing to the small effect of C2 and C6 substituents exchange under neutral conditions.

Experimental Section

Chemicals and steady-state measurements: Isoguanine (IsoG, 95% purity) was purchased from Combi-Blocks, Inc. and was used as received. An aqueous buffer solution at pH 2.4, with a total concentration of 16 mM, was freshly prepared using monosodium phosphate and o-phosphoric acid in ultrapure water. We note that IsoG in its neutral form is not soluble in neutral aqueous buffer solution.[49] Steady-state absorption spectroscopy was performed using a Cary 300 spectrophotometer, with a 300 nm/min scan rate, a data interval of 1.0 nm, and an average time of 0.2 seconds.

Broadband transient absorption spectroscopy: Excited state dynamics were investigated using broadband transient absorption spectroscopy. The transient absorption setup used has been described in detail elsewhere.[51,52,53] TAS spectrometer (Helios, Ultrafast Systems) uses a Ti:Sapphire oscillator (Vitesse, Coherent) that seeds a regenerative amplifier (Libra-HE, Coherent), generating laser pulses centered at 800 nm with a repetition rate of 1 kHz (100 fs). The laser output seeds an optical parametric amplifier (TOPAS, Quantronix/light conversion), tuned to the excitation wavelength of 292 nm for transient absorption measurements. The power of the excitation pulse was set to 0.5 mW. A continuously moving 2 mm CaF_2 crystal was used for white light continuum generation, which gives access to a spectral range from 320 to 700 nm. Fused silica cells with a 2 mm path length were used, with continuous stirring of the solution with a Teflon-coated magnetic stir bar. After completing transient absorption measurements, almost no photodegradation was observed ($< 0.5\%$). No hydrated electron signal of the two-photon ionization of the solvent was detected under the experimental conditions presented in this work.[54] Global and target data analyses were performed using the Glotaran software.[55] The data was globally fit using a two-component sequential model, convoluted with a Gaussian instrument response function of 200 ± 50 fs (FWHM). The EADS were extracted from the global and target analyses.[56]

Computational details: The relative abundance of the tautomers for neutral IsoG in water solution was extracted from the work by Eberlein et al.,[40] whereas for protonated IsoG they were estimated with M06-2X[57]/PCM[58]/6-31G(d,p) following the protocol described in Ref. [40]. For the photophysical study of the protonated and neutral form of IsoG, all the structures were optimized at the MS-CASPT2[59]/SA-8-CASSCF[60](14,11)/ANO-S[61] level of theory using an active space that includes 6π, $4\pi^*$, and 1 n_O orbitals (Schemes S1–S4). Details regarding the absorption spectrum calculations are discussed in the Supporting Information. Absorption spectra at different stationary points of the excited potential energy surface were calculated using the same protocol described above, with

© 2023 The Authors. Chemistry - A European Journal published by Wiley-VCH GmbH

15 roots. Imaginary level[62] and IPEA[63] shifts of 0.30 and 0.25 were respectively used in the MS-CASPT2 calculations. MS-CASPT2 LIICs were employed to connect stationary points. For the calculation of SOC terms, we resorted to the ANO-RCC[64] basis set to include relativistic effects. All the multiconfigurational calculations were performed with OpenMolcas,[65] and Bagel.[66]

Acknowledgements

The authors acknowledge funding from the National Science Foundation (Grant No. CHE-1800052), the Ramón y Cajal Program (Grant: RYC-2016-20489) and the Ministerio de Ciencia, Innovación y Universidades (PGC2018-094644-B-C21, PID2021-125207NB-C31 and PRE2019-090448 projects). L. M. F. thanks the Madrid Government (Comunidad de Madrid-Spain) under the Multiannual Agreement with Universidad Autónoma de Madrid in the line Support to Young Researchers, in the context of the V PRICIT (Regional Programme of Research and Technological Innovation) (SI3/PJI/2021-00331). Thanks are also extended to Red Española de Supercomputación (RES), the Mare Nostrum, Xula and Cesga Supercomputer Centers, and the Centro de Computación Científica of the UAM (CCC-UAM) for the computation time and for their continued technical support.

Conflict of Interest

The authors declare no conflict of interest.

Data Availability Statement

The data that support the findings of this study are available from the corresponding author upon reasonable request.

Keywords: ab initio calculations · excited state dynamics · modified nucleobases · nucleobase ancestors · prebiotic chemistry

[1] A. C. Rios, Y. Tor, *Isr. J. Chem.* **2013**, *53*, 469–483.
[2] S. Ranjan, D. D. Sasselov, *Astrobiology* **2016**, *16*, 68–88.
[3] B. J. Cafferty, N. v. Hud, *Isr. J. Chem.* **2015**, *55*, 891–905.
[4] G. F. Joyce, A. W. Schwartzt, S. L. Millers, L. E. Orgel, *Proc. Nat. Acad. Sci.* **1987**, *84*, 4398–4402.
[5] N. v. Hud, B. J. Cafferty, R. Krishnamurthy, L. D. Williams, *Chem. Biol.* **2013**, *20*, 466–474.
[6] R. Improta, F. Santoro, L. Blancafort, *Chem. Rev.* **2016**, *116*, 3540–3593.
[7] A. A. Beckstead, Y. Zhang, M. S. de Vries, B. Kohler, *Phys. Chem. Chem. Phys.* **2016**,*18*, 24228–24238.
[8] C. E. Crespo-Hernández, B. Cohen, P. M. Hare, B. Kohler, *Chem. Rev.* **2004**, *104*, 1977–2020.
[9] T. Gustavsson, R. Improta, D. Markovitsi, *J. Phys. Chem. Lett.* **2010**, *1*, 2025–2030.
[10] M. P. Callahan, K. E. Smith, H. James, C. li, J. Ruzicka, J. C. Stern, D. P. Glavin, C. H. House, J. P. Dworkin, *Proc. Nat. Acad. Sci.* **2011**, *108*, 13995–13998.
[11] H. L. Barks, R. Buckley, G. A. Grieves, E. di Mauro, N. v. Hud, T. M. Orlando, *ChemBioChem* **2010**, *11*, 1240–1243.
[12] R. Hayatsu, *Science* **1964**, *146*, 1291–1293.
[13] A. Eschenmoser, E. Loewenthal, *Origins Life Evol. Biospheres* **1992**, *24*, 1–16.
[14] Y. A. Jeilani, B. Ross, N. Aweis, C. Fearce, H. Minh Hung, M. T. Nguyen, *J. Phys. Chem. A* **2018**, *122*, 2992–3003.
[15] Y. A. Jeilani, H. T. Nguyen, B. H. Cardelino, M. T. Nguyen, *Chem. Phys. Lett.* **2014**, *598*, 58–64.
[16] C. Roberts, J. C. Chaput, C. Switzer, *Chem. Biol.* **1997**, *4*, 899–908.
[17] H. J. Cleaves, in *Prebiotic Chemistry and Chemical Evolution of Nucleic Acids. Nucleic Acids and Molecular Biology*, Vol. 35 (Eds: C. Menor-Salván), Springer, Madrid, Spain **2018**, Ch. 16.
[18] H. Kamiya, *Nucleic Acids Res.* **2003**, *31*, 517–531.
[19] H. Kamiya, H. Kasai, *J. Biol. Chem.* **1995**, *270*, 19446–19450.
[20] N. Murata-Kamiya, H. Kamiya, M. Muraoka, H. Kaji, H. Kasai, *J. Radiat. Res.* **1997**, *38*, 121–131.
[21] P. Di Mascio, G. R. Martínez, S. Miyamoto, G. E. Ronsein, M. H. G. Medeiros, J. Cadet, *Chem. Rev.* **2019**, *119*, 2043–2086.
[22] J. A. Piccirilli, T. Krauch, S. E. Moroney, S. A. Benner, *Nature* **1990**, *343*, 33–37.
[23] S. Hoshika, N. A. Leal, M.-J. Kim, M.-S. Kim, N. B. Karalkar, H.-J. Kim, A. M. Bates, N. E. Watkins, H. A. Santalucia, A. J. Meyer, S. Dasgupta, J. A. Piccirilli, A. D. Ellington, J. Santalucia, M. M. Georgiadis, S. A. Benner, *Science* **2019**, *363*, 884–887.
[24] C. Roberts, R. Bandaru, C. Switzer, *J. Am. Chem. Soc.* **1997**, *119*, 4640–4649.
[25] G. Gate, R. Szabla, M. R. Haggmark, J. Šponer, A. L. Sobolewski, M. S. de Vries, *Phys. Chem. Chem. Phys.* **2019**, *21*, 13474–13485.
[26] N. E. Caldero-Rodríguez, C. E. Crespo-Hernández, *Phys. Chem. Chem. Phys.* **2022**, *24*, 6769–6781.
[27] K. N. Rogstad, Y. H. Jang, L. C. Sowers, W. A. Goddard, *Chem. Res. Toxicol.* **2003**, *16*, 1455–1462.
[28] J. R. Blas, F. J. Luque, M. Orozco, *J. Am. Chem. Soc.* **2004**, *126*, 154–164.
[29] G. Maheen, Y. Wang, Y. Wang, Z. Shi, G. Tian, S. Feng, *Heteroat. Chem.* **2011**, *22*, 186–191.
[30] J. Kua, J. L. Bada, *Origins Life Evol. Biospheres* **2011**, *41*, 553–558.
[31] A. Albert, D. J. Brown, *J. Chem. Soc.* **1954**, 2060–2071.
[32] S. F. Mason, *J. Chem. Soc.* **1954**, 2071–2081.
[33] R. M. C. Dawson, D. C. Elliott, W. H. Elliott, K. M. Jones, in *Data for Biochemical Research*, **1986**, pp. 6–7.
[34] M. A. El-Sayed, *J. Chem. Phys.* **1963**, *38*, 2834–2838.
[35] M. A. El-Sayed, *J. Chem. Phys.* **1962**, *36*, 573–574.
[36] J. M. L. Pecourt, J. Peon, B. Kohler, *J. Am. Chem. Soc.* **2000**, *122*, 9348–9349.
[37] J. M. L. Pecourt, J. Peon, B. Kohler, *J. Am. Chem. Soc.* **2001**, *123*, 10370–10378.
[38] P. M. Hare, C. E. Crespo-Hernández, B. Kohler, *J. Phys. Chem. B* **2006**, *110*, 18641–18650.
[39] P. M. Hare, C. E. Crespo-Hernández, B. Kohler, *Proc. Nat. Acad. Sci.* **2006**, *104*, 435–440.
[40] L. Eberlein, F. R. Beierlein, N. J. R. van Eikema Hommes, A. Radadiya, J. Heil, S. A. Benner, T. Clark, S. M. Kast, N. G. J. Richards, *J. Chem. Theory Comput.* **2020**, *16*, 2766–2777.
[41] L. Serrano-Andrés, M. Merchán, A. C. Borin, *J. Am. Chem. Soc.* **2008**, *130*, 2473–2484.
[42] S. Yamazaki, W. Domcke, A. L. Sobolewski, *J. Phys. Chem. A* **2008**, *112*, 11965–11968.
[43] R. González-Luque, T. Climent, I. González-Ramírez, M. Merchán, L. Serrano-Andrés, *J. Chem. Theory Comput.* **2010**, *6*, 2103–2114.
[44] M. Pollum, L. Martínez-Fernández, C. E. Crespo-Hernández, in *Photo-induced Phenomena in Nucleic Acids I Nucleobases in the Gas Phase and in Solvents* (Eds: M. Barbatti, A. C. Borin, S. Ullrich), Springer Charm, Switzerland, **2014**, Ch. 7.
[45] C. E. Crespo-Hernández, B. Cohen, P. M. Hare, B. Kohler, *Chem. Rev.* **2004**, *104*, 1977–2020.
[46] V. Karunakaran, K. Kleinermanns, R. Improta, S. A. Kovalenko, *J. Am. Chem. Soc.* **2009**, *131*, 5839–5850.
[47] T. Fujiwara, Y. Kamoshida, R. Morita, M. Yamashita, *J. Photochem. Photobiol. B* **1997**, *41*, 114–121.
[48] J. Peon, A. H. Zewail, *Chem. Phys. Lett.* **2001**, *348*, 255–262.
[49] K. Dybiec, A. Gryff-Keller, *Pol. J. Chem.* **2006**, *80*, 1831–1843.
[50] C. Reichardt, R. A. Vogt, C. E. Crespo-Hernández, *J. Chem. Phys.* **2009**, *131*, 10.1063/1.3272536.
[51] C. Reichardt, C. Wen, R. A. Vogt, C. E. Crespo-Hernández, *Photochem. Photobiol. Sci.* **2013**, *12*, 1341–1350.
[52] M. Pollum, S. Jockusch, C. E. Crespo-Hernández, *J. Am. Chem. Soc.* **2014**, *136*, 17930–17933.

© 2023 The Authors. Chemistry - A European Journal published by Wiley-VCH GmbH

[53] M. M. Brister, C. E. Crespo-Hernández, *J. Phys. Chem. Lett.* **2019**, *10*, 2156–2161.
[54] C. E. Crespo-Hernández, B. Kohler, *J. Phys. Chem. B* **2004**, *108*, 11182–11188.
[55] J. J. Snellenburg, S. P. Laptenok, R. Seger, K. M. Mullen, I. H. M. van Stokkum, *J. Stat. Soft* **2012**, *49*.
[56] I. H. M. van Stokkum, D. S. Larsen, R. van Grondelle, *Biochim. Biophys. Acta Bioenerg.* **2004**, *1657*, 82–104.
[57] Y. Zhao, D. G. Truhlar, *Theor. Chem. Acc.* **2008**, *120*, 215–241.
[58] M. Cossi, V. Barone, R. Cammi, J. Tomasi, *Chem. Phys. Lett.* **1996**, *255*, 327–335.
[59] K. Andemson, P.-A. Malmqvist, B. O. Roos, A. J. Sadlej, K. Wolinskit, *J. Phys. Chem.* **1990**, *94*, 5483–5488.
[60] B. O. Roos, in *The Multiconfigurational (MC) Self-Consistent Field (SCF) Theory. Lecture Notes in Quantum Chemistry. Lecture Notes in Chemistry, 58*. Springer: **1992** Berlin, Heidelberg.
[61] P. Å. Widmark, P. Å. Malmqvist, B. O. Roos, *Theor. Chim. Acta* **1990**, *77*, 291–306.
[62] N. Forsberg, A. Malmqvist, *Chem. Phys. Lett.* **1997**, *274*, 196–204.
[63] G. Ghigo, B. O. Roos, P. Å. Malmqvist, *Chem. Phys. Lett.* **2004**, *396*, 142–149.
[64] B. O. Roos, R. Lindh, ke Malmqvist, V. Veryazov, P.-O. Widmark, *J. Phys. Chem. A* **2004**, *108*, 2851–2858.
[65] I. Fdez. Galván, M. Vacher, A. Alavi, C. Angeli, F. Aquilante, J. Autschbach, J. J. Bao, S. I. Bokarev, N. A. Bogdanov, R. K. Carlson, L. F. Chibotaru, J. Creutzberg, N. Dattani, M. G. Delcey, S. S. Dong, A. Dreuw, L. Freitag, L. M. Frutos, L. Gagliardi, F. Gendron, A. Giussani, L. González, G. Grell, M. Guo, C. E. Hoyer, M. Johansson, S. Keller, S. Knecht, G. Kovačević, E. Källman, G. Li Manni, M. Lundberg, Y. Ma, S. Mai, J. P. Malhado, P. Å. Malmqvist, P. Marquetand, S. A. Mewes, J. Norell, M. Olivucci, M. Oppel, Q. M. Phung, K. Pierloot, F. Plasser, M. Reiher, A. M. Sand, I. Schapiro, P. Sharma, C. J. Stein, L. K. Sørensen, D. G. Truhlar, M. Ugandi, L. Ungur, A. Valentini, S. Vancoillie, V. Veryazov, O. Weser, T. A. Wesołowski, P. O. Widmark, S. Wouters, A. Zech, J. P. Zobel, R. Lindh, *J. Chem. Theory Comput.* **2019**, *15*, 5925–5964.
[66] T. Shiozaki, Wiley Interdiscip. Rev. Comput. Mol. Sci. **2018**, *8*, 1331.

Manuscript received: November 17, 2022
Accepted manuscript online: January 24, 2023
Version of record online: ■■, ■■

© 2023 The Authors. Chemistry - A European Journal published by Wiley-VCH GmbH

RESEARCH ARTICLE

Combined transient absorption spectroscopy and quantum mechanical calculations reveal the photophysical feasibility of isoguanine as a nucleobase precursor under prebiotic conditions. Protonated isoguanine decays to the ground state in sub-ps time scales, consistently with the barrierless potential energy profiles connecting the Franck-Condon region with internal conversion funnels.

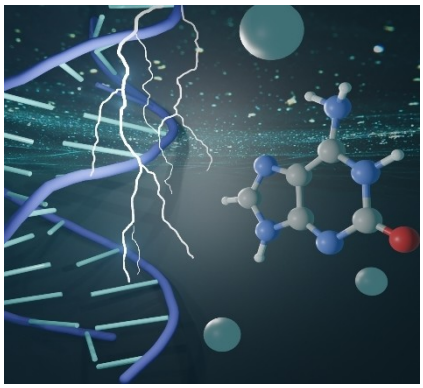

J. Ortín-Fernández, Dr. N. E. Caldero-Rodríguez, Dr. C. E. Crespo-Hernández, Dr. L. Martínez-Fernández*, Dr. I. Corral**

1 – 10

Photophysical Characterization of Isoguanine in a Prebiotic-Like Environment